Predicting Schrödinger's range-shifting cat: Analytic results for the impact of asymmetric environmental dependence on species responses to climate change

J. Christopher D. Terry[1,(corresponding)], Jacob D. O'Sullivan[1], and A. G. Rossberg[1]

February 4, 2022

[Preliminary draft - further updates are planned before journal submission]

Affiliations: [1]School of Biological and Behavioural Sciences, Queen Mary University of London, Mile End Road, London, E1 4NS, United Kingdom

Abstract

Analytic models for how species will respond to climate change can highlight key parameter dependencies. By mapping equations for population dynamics onto corresponding problems from quantum mechanics with known solutions we derive analytical results for the frequently observed case of asymmetric environmental response curves. We derive expressions in terms of parameters representing climate velocity, dispersal rate, maximum growth rate, niche width, high-frequency climate variability and environmental performance curve skew for three key responses: 1) population persistence, 2) lag between range displacement and climate displacement, 3) location of maximum population sensitivity. Surprisingly, under our model assumptions, the direction of performance curve asymmetry does not strongly contribute to either persistence or lags. A simple metapopulation simulation corroborated this result. Measures to support range-shifting populations may have most benefit where the environmental dependence is shallow, irrespective of whether this is the 'leading' or 'trailing' edge. Our results introduce new tools to ecology and illustrate the continued role of analytic theory.

1 Introduction

Climate change is causing shifts in the ranges of many species (Parmesan & Yohe 2003; Lenoir et al. 2020) and improving capacity to understand the complex ecological dynamics underlying these movements and to better forecast range shifts is crucial to conservation efforts (Urban et al. 2016). Range shifts are not instantaneous, leading to communities that are increasingly out of equilibrium with their climatic niche (Svenning & Sandel 2013; Alexander et al. 2018; Rumpf et al. 2019; Lenoir et al. 2020). For species that have narrow environmental niches, persistence is determined by the rate of extirpation from sites at its trailing edge, and the colonisation rate at its leading edge (Kerr 2020). As such, while species-distribution models (Elith & Leathwick 2009) can be informative of the potential end state after a certain amount of climate change, dynamic models are needed to capture the processes by which a species range may shift through time (Zurell et al. 2009, Alexander et al. 2017). To meet this need, a large number of modelling approaches have been applied to this topic, spanning the full breadth of the possible trade-offs between model precision, realism and specificity.

The most involved non-specific approach is to attempt to model as many processes as practically possible in large generalised spatially-explicit simulation models (e.g. Brooker et al. 2007; Urban et al. 2012; Lurgi et al. 2015; Thompson & Gonzalez 2017; Thompson & Fronhofer 2019). These approaches are very flexible, but insights are fundamentally limited to illustrating potential cases within the parameter and model structure examined in any particular study. Results can depend strongly on the underlying assumptions of the model (Zurell et al. 2016). Further, the complexity of these models makes the systematic interrogation of conclusions drawn from particular parameter choices a challenge. More abstracted approaches using moving-habitat integro-differential equation (IDE) models (Zhou & Kot 2011; Kot & Phillips 2015; Harsch et al. 2017; Hurford et al. 2019) that include a continuous spatial element and a discrete temporal component can capture many nuances of dispersal processes and are somewhat analytically tractable (Kot & Phillips 2015) but results are still largely limited to the inspection of simulation results.

There is still a strong need for fundamental theoretical research to identify critical features. Purely analytic models provide another perspective to the problem, providing an 'all-else-equal'

baseline for consideration. To fill this gap, partial differential equation models building on well-established reaction-diffusion equations (Cantrell & Cosner 2003) models for invasive species and the spread of genes (Fisher 1937; Skellam 1951; Hastings et al. 2005), have been applied to climate change scenarios (Pease et al. 1989; Potapov & Lewis 2004; Berestycki et al. 2009; Li et al. 2014). This work has been able to identify the critical rate of climate change that a species can adequately respond to as being a function of the dispersal rate and the growth of the population when rare, allowing the direct comparison with data (Leroux et al. 2013).

However, to date, these analytic models have been restricted to simple representations of species performance across environments using symmetric functions. It is widely appreciated that almost all species show asymmetric environment-performance curves (EPC, Savage et al. 2004), most commonly characterised by a slow increase in performance to an optimum followed by a relatively sharp decline (illustrated in Fig 2). Disparities in environmental sensitivity between the trailing and leading edges of species range may be expected to influence its range-shift dynamics. For example, using a numerical IDE approach Hurford et al. (2019) demonstrated a case where the skew of a species EPCs and dispersal interact to cause divergent effects depending on the direction of the asymmetry. Further, these asymmetries may be particularly relevant when underlying climatic variability is also considered (Nadeau et al. 2017).

Here, we extend previous analytic theory to incorporate asymmetric environmental dependence and use this theory to directly investigate the impact of this asymmetry on three key properties: likelihood of persistence, range-shift lag and the location of peak sensitivity to conservation interventions. We do this by framing the species-movement problem as a Schrödinger equation, unlocking mathematical results from the quantum mechanics literature. Under the assumptions of our model, we show that the direction of the skew is not influential in terms of either a proxy for extinction risk or lags in range shifts. We corroborate these results in a model simulation exhibiting complex dynamics and discuss how they could aid the interpretation of empirical observations.

2 Analytic Theory

2.1 Setting and specification of core model

For lucidity we only outline the mathematical derivations here, restricting full details to the Appendices where we also include an evaluated Mathematica notebook to replicate our analysis and results. Throughout, we assume a system with a single spatial dimension (x) that spans a linear gradient in an environmental variable E. For simplicity we set initial values of $E = x$. Our E could represent any environmental variable, but is most easily conceptualised as an average temperature at a particular location. Climate change is introduced by a linear time dependence of E: $E_{x,t} = x - vt$, where v is the rate of change in E due to climate change. By this formulation, the location where $E = 0$, moves along the x-axis with velocity v. If taken to represent 'polewards' movement of species, x could represent latitude or, at local scales, elevation. The direct correspondence between space and the environmental variable E means that this v can also be directly interpreted as a 'climate velocity' with units of *distance* t^{-1} (Brito-Morales et al. 2018).

A species local population growth rate at each point in space is defined by an environmental performance curve (EPC) function $g(E)$. We then define a generic partial-differential equation expression (e.g. Fisher 1937, Hastings et al. 2005) for the change through time of a population (u) across space and time, including dispersal as:

$$\frac{\partial u(x,t)}{\partial t} = g(E_{x,t})u(x,t) \ + D\frac{\partial^2 u(x,t)}{\partial x^2} \tag{1}$$

Since we are especially interested in the dynamics of vulnerable populations we assume that the population density is at all times small relative to its potential carrying capacity. We do not therefore model density dependence in growth rates. Any density-dependence would affect the resultant population growth rates and absolute equilibrium population size, but importantly not the overall functional form of solutions at or close to the steady state which we are most interested in. See Appendix 1.3 for further discussion on this point.

The effect of migration in and out of the local population at a particular location is incorporated via a dispersal rate term D, the mean squared displacement of population in units of

time. The rate of net migration is based on the curvature of the population density to either side of the focal population. This results in populations near the central peak of the biomass distribution (where the population density curvature is convex) losing population density to net-migration, while the tails of the distribution (where the curvature is concave) gaining. Defined in this way, D can be directly related to the mean movement of individuals per generation (Kareiva & Shigesada 1983).

Central to our approach is a change of reference frame to track the movement of suitable habitat across the landscape. We do this by defining $y = x - vt$, and using y as our principal spatial variable (Fig 1). This allows us to examine the distribution of the population with reference to the total environmental displacement that has occurred due to climate change. Evaluation of the derivatives results in the core partial differential equation:

$$\frac{\partial u(y,t)}{\partial t} = g(E_{y,t})u(y,t) \ + D\frac{\partial^2 u(y,t)}{\partial y^2} + v\frac{\partial u(y,t)}{\partial y} \tag{2}$$

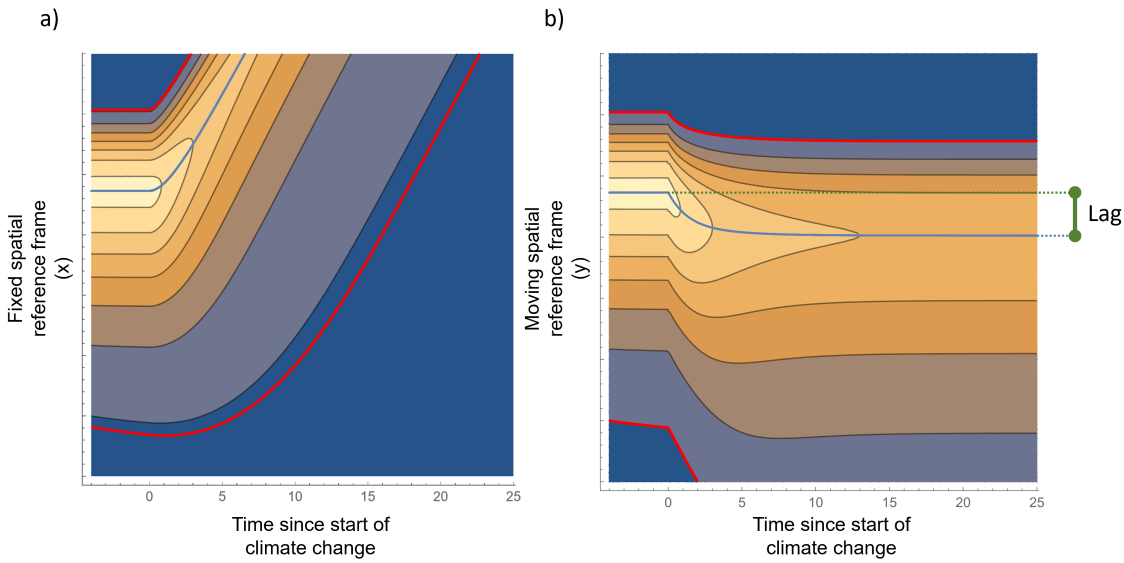

Figure 1: A) Example of movement of species range with climate change under a fixed spatial reference frame (x). Climate change (v) shifts is set to +0.45 starting at t=0 (movement before $t = 0$ is just slight out-of equilibrium progression). Brightness of colour signifies population density, peak density is indicated by the central blue line. B) Species range through time under climate change in the moving reference frame (y) - parameters are otherwise identical to a). With ongoing climate change, after a period of adjustment the population reaches a steady travelling wave state, with a lower overall population density and a constant lag behind the moving climate. Parameter values are given in the Mathematica supplement

	Term	Meaning
Core Model Terms	x	Spatial coordinate
	v	Rate of climate change
	y	Spatial location, reference frame adjusted for climate change $y = x - vt$
	$u(y,t)$	Population density at point y and time t
	E	Environmental variable
	$g(E)$	Environmental performance curve (EPC) function describing local population growth rate given E
	$\psi(y,t)$	Function that describes population distribution across space and time.
	λ	Population growth rate
	λ_0	Population growth rate, without climate change
	D	Dispersal rate
EPC parameters	w	Niche width parameter
	a	Asymmetry of EPC
	ϕ	Environmental optimum, and peak of $g()$
	R_{max}	Growth rate at optimum
	σ	SD of temporal environmental variation
Derived Values	v^*	Critical rate of climate change at which the population cannot persist ($\lambda = 0$)
	Δ	Lag in space between total climate displacement and displacement of population at steady state
	S_{max}	Location of peak sensitivity of λ, relative to optimum

Table 1: Summary of parameters and variables used in the analytic models.

2.2 Formulation as a Schrödinger Equation

To describe this core model in a more useful way, we next specify:

$$u\left(y,t\right) = e^{\lambda t} \times \psi\left(y,t\right) \tag{3}$$

This defines how the biomass at any particular point in time $u\left(y,t\right)$ in terms of the total population increase ($e^{\lambda t}$, where λ corresponds to the long-term growth rate), and a new function $\psi(y,t)$, that describes the overall shape of the population distribution across space at a particular time. While it can be directly solved for, it is very complex in form. However, by inserting Eq. (3) into Eq. (2), evaluating the derivatives, and rearranging, we can reach:

$$\left(\lambda + \frac{v^2}{4D}\right)\psi(y,t) = g(y)\psi(y,t) + D\frac{d^2\psi(y,t)}{dy^2}, \tag{4}$$

Further progress in understanding range shifts under environmental change can be made by noting that Eq. (4) has the same form as the time-independent Schrödinger equation (Schrödinger, 1926) for the wave function ψ of a particle moving in a one-dimensional energy potential $V(y)$:

$$E\psi = V(y)\psi - \frac{\hbar^2}{2m}\frac{d^2\psi}{dy^2}, \tag{5}$$

where in this case E denotes the total energy and the last term represents the kinetic energy of a particle with mass m. Comparing terms, one sees that the potential $V(y)$ corresponds to the negative performance environmental function $-g(y)$ (see also S1.6). The non-negative solution for ψ studied here corresponds to the lowest-energy ('base') state of the quantum-mechanical system. Although this expression may not look particularly informative on its own (indeed, Schrödinger functions are statements of fact, rather than results as such), by describing the relationships between a large number of key elements relevant to range changes, it is possible to derive a large number of informative results since Equation (5) has been studied extensively. This has led not only to a strong body of intuition about the nature of the solutions of the eigenvalue problem given by Eq. (5), but also the discovery of a range of functional forms for the potential $V(y)$ for which closed-form solutions of this problem can be derived (Mattis 1993).

Importantly, this does not mean that we must adopt the probabilistic elements of quantum mechanics, but can help unlock additional existing mathematical results from the quantum mechanics literature. Note that we only consider real valued-solutions and so the resultant approach is very closely related to the classic reaction-diffusion model approach (Nagasawa 1993).

2.3 Representing Environmental Performance Curves

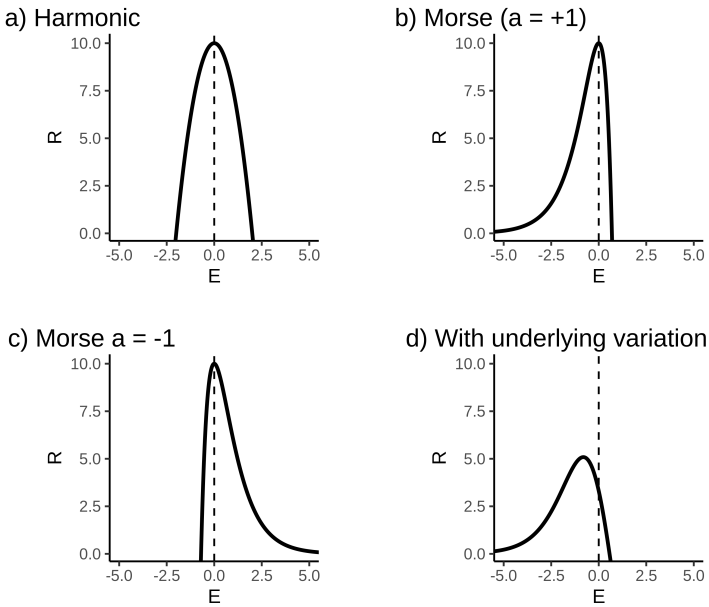

Figure 2: Illustration of environmental performance curves under different models that can be analysed analytically. In each case the species has an optimum $\phi = 0$ and $R_{max} = 10$ a) harmonic potential function, $w = 2$. b) Morse potential function, where $a = +1$, $w = 1$ c) Morse potential function $a = -1$, $w = 1$, d) Morse potential function as ii), but incorporating the effects of a variable E, (mean 0, sd = 1). Note how with the peak of the curve has shifted with the introduction of noise.

The function $g(E)$ describes the species performance under different environmental conditions can be defined as any differentiable function that accepts all real numbers, and the equation numerically solved. However, by selecting one of the many functions that have been analytically solved (for an accessible list see `http://wikipedia.org/wiki/List_of_quantum-mechanical_systems_with_analytical_solutions`) the analytical possibilities are considerably broadened. For example, a harmonic potential function defines a symmetric environmental performance curve (Fig 1a) as:

$$g_{har}(E) = R_{max}\left(1 - \frac{(E - \phi)^2}{w^2}\right) \tag{6}$$

where R_{max} is growth rate of the species at its optimum ϕ, and w is a niche width parameter.

For simplicity we will assume $\phi = 0$ throughout. An asymmetric environmental performance curve (Fig 1b,c) can be defined using a Morse potential (Morse 1929) function:

$$g_{Mor}(E) \;=\; R_{max}\left(1 - \frac{\left(1 - e^{a(E-\ \phi)}\right)^2}{a^2 w^2}\right) \tag{7}$$

which includes an additional non-zero asymmetry parameter a. For comparison with other functions, this term can related to the derivatives of $g()$ at the peak of the curve: $a = g'''(\phi)/3g''(\phi)$.

Care needs to be taken with the naming of skew direction - a *positive* value of a leads to a 'negative' or left-tailed skew (Fig 1b,c) in terms of E (and so our x). If E represented a temperature variable that increased through time with climate change (remembering that positive E and x values are the direction of climate velocity, and hence cooler) a positive a value would typically be described as a 'warm-skewed' growth curve, because the heavy tail is to the warmer (more equatorial, lower elevation) side of the optimum (Hurford et al. 2019).

On top of these underlying functions, the effect of high-frequency temporal environmental variation can be introduced by convolving these curves with a probability density function that represents the environmental variance. When environmental variability is represented by a Normal distribution with standard deviation σ, the convolution changes the shape, but not the underlying form of the performance function. Hence, a harmonic potential maps onto a harmonic potential and the Morse potential onto a Morse potential, although in both cases with modified shape. In Fig 1d, we show the effect of introducing $\sigma = 1$ on the overall effective environmental performance curve, acting to soften the edges as well as shifting and flatten the peak of the distribution.

3 Analytic Results

We use our model to find analytic results for how three key response properties depend on model parameters – 1) the capacity for a species to be able to sustain itself under a climate change scenario, 2) the lag between where the distribution of a species 'should' be if it perfectly kept pace with climate change and where it actually is, and 3) the location of peak sensitivity where conservation interventions would be most efficacious.

3.1 Response 1: Critical speed of climate change

In Eq. (4), λ represents the growth rate of the population. When λ is positive, the species is able to expand its population size from rare, and we can say that the population is likely to resist extinction due to climate change. By first denoting the population growth rate of the species without climate change (i.e. $v = 0$) as λ_0, then we can directly find (S1.4) that once climate change is introduced and the travelling system is at an equilibrium (i.e. the shape of the population distribution in the moving reference frame has stabilised) that the resultant growth population growth rate is simply:

$$\lambda = \lambda_0 - \frac{v^2}{4D} \tag{8}$$

where, remarkably the decline in fitness can be seen to be entirely independent of the form of the environmental performance curve function $g()$. Also of interest is that the impact of climate change rate on population fitness is quadratic, predicting that there may be a relatively sharp threshold where the pace of range shifting required for a population to persist is too much.

This expression can be rearranged to determine the critical speed of climate change (v^*), beyond which the species can no longer keep up and will inevitably go extinct:

$$v^* = \sqrt{\lambda_0 - 4D\lambda} \tag{9}$$

A final rearrangement, to solve for D, can identify the critical rate of dispersal that a species must exceed in order to maintain its population (Hastings et al. 2005; Leroux et al. 2013). This is also not directly dependent of the shape of $g()$.

The shape of the curve does however influence the initial population growth rate (λ_0). For example, using the asymmetric environmental performance curve defined above, we can solve (B.Response 1) for the relatively simple expression that defines the population growth rate in terms of key model parameters:

$$\lambda \quad = R_{max} - \frac{v^2}{4D} - \frac{\sqrt{DR_{max}}}{w} + \frac{a^2 D}{4} \tag{10}$$

which holds as long as $D < 4R_{max}/a^4w^2$.

The first three terms of Eq. (10) re-derive previously known results (Pease et al. 1989) about the impact of climate change in the case of a symmetric (Gaussian) EPC. Reassuringly, the model predicts that 1) that a greater maximum population growth rate increases fitness and 2) that faster climate change is detrimental to population fitness. The effect of dispersal rate D is multifaceted – the second term shows how greater dispersal can directly offset the impact of faster climate change, but the third term shows a negative effect of greater dispersal due to losses from the central part of the population. This last effect is mitigated by larger niche widths.

The fourth term predicts that the impact of asymmetry acts quadratically, and is therefore not dependent on the direction of the skew – whether the precipitous decline in fitness is on the leading or trailing edge of the species range is not relevant to the initial population fitness. This follows naturally from the result that asymmetry only influences the baseline population fitness, which does not have any sense of directionality. Comparison with (8) shows that most of the terms of (10) can be identified as contributing only to initial λ_0 component, not the response to climate change *per-se*.

Similarly, the effect of high-frequency temporal variation in our model is represented by changes in the form of $g()$, and so can be shown to not alter the impact of climate change ((8),(9)). That said, σ) does impact the overall expression for λ in a complex manner (Appendix B). The marginal effect of increasing σ on λ is easier to interpret:

$$\frac{d\lambda}{d\sigma} = \frac{wa^2\sqrt{DR_{max}} - 2R_{max}}{w^2} \tag{11}$$

and shows that the marginal effect of temporal variation on fitness is dependent on a large number of model terms. The quadratic range width denominator suggests that temporal variation is most influential with narrow ranged species, but the overall effect depends on a balance of many parameters. Asymmetry and dispersal both increase the positive aspects of environmental variation, but again the direction of the asymmetry is not relevant.

3.2 Response 2: Range shift lag behind climate change

Since species take time to respond to climate change, there is expected to be a measurable lag (in space and time) between how the climate has changed and the distribution of the population (Alexander et al. 2018). With a constant rate of climate change, and assuming the population is able to maintain itself, a population will reach an equilibrium state of a static travelling wave. Even in an idealised model system like ours, there are multiple metrics that can be used to describe a species range in space (Yalcin & Leroux 2017). Here we measure lag (Δ) as the difference between the peak of the population density distribution and the location of the optimum environment at this travelling wave stage (Figure 1).

Using the asymmetric growth rate function including the effect of temporal variation, we can derive expressions for this lag (Appendix B). Here we focus on the case where the rate of climate change v is relatively small, the steady-state lag converges on:

$$\Delta \rightarrow \frac{w}{2\sqrt{DR_{max}}} + \frac{a^2 w \left(\sigma^2 \sqrt{DR_{max}} + 2Dw\right)}{4DR_{max}} \tag{12}$$

If 'lag' is instead measured the shift location of the centre of mass of the population density, very similar results can be found (Appendix B). Where there is no asymmetry ($a = 0$), only the first term is relevant. The denominator of the first term reaffirms the intuition that lags are reduced by greater dispersal and larger maximum growth rates. The numerator shows that lags are predicted to be greater when niche widths are wider – essentially the population does not need to move with as much alacrity when a larger part of the environment is suitable.

From the second term of Eq 12, where there is asymmetry ($a \neq 0$), the exact impact interacts in a complex way with other parameters but greater asymmetry always increases the lag. To a first approximation this depends only on the magnitude of asymmetry, not the sign. The effect of σ is tied to the asymmetry of the EPC, with variation combining with asymmetry to increase the lag, while in the symmetric case, the σ has no effect.

3.3 Response 3: Sensitivity to Conservation Actions

Our model can be analysed to examine which area is most consequential to the overall population growth rate, and might therefore be of particular conservation priority. We do this by assessing the sensitivity of λ to population perturbations at different points in space. Note that we maintain using the moving spatial reference frame y, so that locations are relative to the environmental optimum at each point in time as climate change progresses. This method is analogous to determining the most sensitive life-stage of a population (e.g. Caswell 2012, 2019), but substituting age for space. The sensitivity of λ is proportional to the product of the reproductive value and the abundance at each environment in the stable distribution.

By solving for the location of the peak sensitivity relative to the optimum environment (i.e. y), we can find:

$$S_{max} = \frac{1}{a} \ln \left[1 - a^2 \sqrt{\frac{D}{4R_{max}}} \right] \tag{13}$$

which holds for moderate levels of asymmetry ($a^2 w \sqrt{\frac{D}{R_{max}}} < 2$).

Because the value inside the logarithm is always less than 1, this means that the sign S_{max} depends solely on the direction of the asymmetry, always occurring on the long-tail side of the environmental optimum (Figure 3), irrespective of the direction of climate change. In Appendix 1.5, we show that this direction-independence is a highly general result not dependent on the functional form of the EPC.

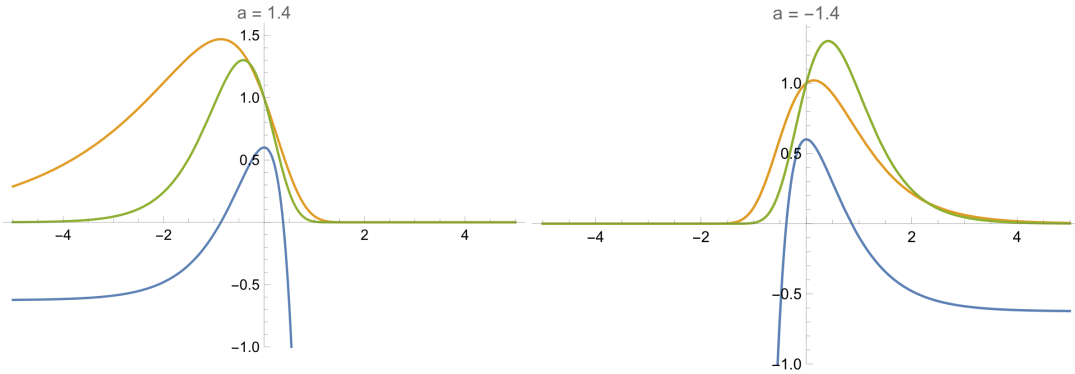

Figure 3: Distribution of sensitivity and population density dependent on underlying EPC at the travelling wave state. In both panels, the horizontal axis is in y, the species leading edge is to the right, and the trailing edge to the left. Apart from the asymmetry of the EPC, parameters are the same. only the direction of asymmetry varies. Horizontal axis $= y$, the moving reference frame where $0 =$ the species environmental optimum. Three quantities plotted: EPC function, showing environmental optima at $y = 0$ (blue), population density (ψ, orange, standardised to equal 1 at $y = 0$),and sensitivity (also scaled, Green).

4 Comparison with simulations

In order to derive these analytic results, our framework makes a number of significant simplifying assumptions. To test the translatability of predictions made by our model to more complex systems, we built a spatially-explicit population model. Expanding on the continuous-time and continuous space analytic results, we built this model to include randomness and discreteness in both space and time, as well as carrying capacities for each species.

4.1 Model Specification

Full details of our simulation model are given in Appendix C, and all code is available as described in the data accessibility statement. Briefly, we generated rectangular arenas with dimensions 10x40, each with 200 randomly located discrete nodes connected to their nearest neighbours (Figure 4a). A single environmental variable linearly increases along the x-axis of each arena from 0 to 40. To represent temporal environmental variability, for each set of 15 timesteps (which we refer to as a 'year') we drew added a value drawn from Gaussian distribution with mean 0 and standard deviation 0.5 to all environmental values during that year.

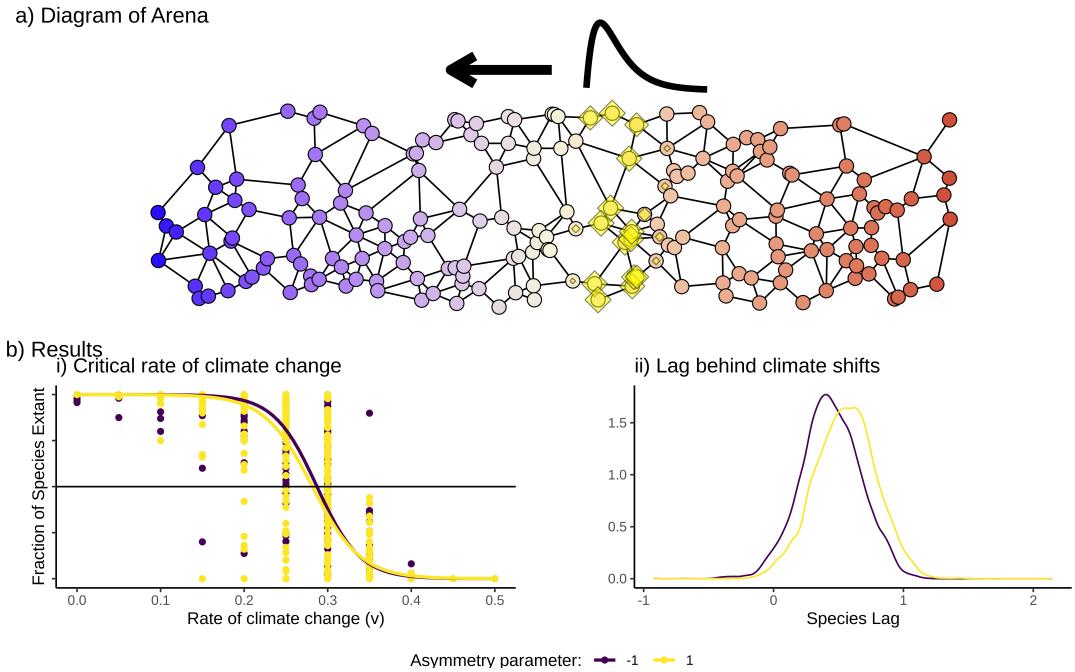

Figure 4: **Metapopulation simulations setting and results** a) Illustration of example virtual region of connected habitats the species inhabit in the simulation. Initial mean environmental values (E) are given by the blue (low) to red (high) colouration. The size of the yellow diamonds illustrates the population density at each site. The environmental performance curve of the species (right-skewed, $a = -1$) is drawn above. With climate change and an increasing underlying environmental variable, the species will have to shift its range leftwards. b) Numerical results from the simulations, partitioned by the direction of the skew of the EPC illustrating its small influence i) The speed of climate change (v) at which the proportion of species that are able to survive falls below 0.5. Lines are fitted binomial GLMs. ii) density plots of the lag by which species fall behind the movement of climate and a moderate rate of climate change.

Population dynamics of each species were modelled in discrete time and followed logistic growth with dispersal between nodes, where the intrinsic growth rate R_{max} depended on the current environment at that node through performance functions based on eq 6, with $R_{max} = 10$, $w = 1$ and $a = +/-1$). Immigration into neighbouring sites was determined by an exponential distance decay function, with a level of total dispersal chosen such that extinctions are possible once climate change is introduced.

Initially, 100 species were generated with environmental optima (ϕ) drawn from a uniform distribution between 20 and 30. These species will maintain a region of suitability at the end of the simulation and so are less affected by possible edge effects. The arenas were seeded with initial colonists and the model integrated for 200 'years' to fill their initial range. Species that

fell below a threshold biomass (10^{-6}) across all nodes were considered extinct and removed.

We assembled 100 sets of species with either direction of environmental performance skew ($a = +1$ or -1). We do not test a symmetric environmental performance curve case, as it is not possible to standardise all aspects of the performance curve for a fair comparison. We examined two response metrics that could be derived from both the simulation model and the analytic model, to assess if the pattern of parameter dependencies holds.

4.2 Critical rate of climate change

We sequentially simulated each assembled set of species under varying rates of climate chance ($v = 0$ to 0.5 in steps of 0.05) and identified the fraction of species that had fallen below 1% of their starting total population size at the end of 50 'years' of climate change. In line with our expectations, there was a relatively precipitous decline in survival chance. Both a = +1 and -1 showed very similar responses (Figure 4bi). We fit a generalised linear mixed-effects model that included as main predictors v, a, their interactions and assemblage as a random effect to estimate the v at which the 50% of species go extinct. When left-skewed, $v_{50} = 0.281$, while when right-skewed,$v_{50} = 0.287$.

4.3 Movement Lags

We tested the lag in movement of the centre of mass of the population distribution for each of the assemblies at a moderate climate change rate. We assessed the starting average location of the 'centre of mass' of each species before any climate change (${m_i}^{\text{start}}$) as the average x-coordinate of each node, weighted by the biomass of species i at each node, averaged over 20 years. We then ran 70 years of climate change at $v = 0.1$, and measured the average lag ($\bar{\Delta}_i$) for each species over final 20 years:

$$\bar{\Delta}_i = \frac{1}{20} \sum_{t=51}^{70} \left(m_i^{\text{start}} + vt - m_{i,t} \right) \tag{14}$$

Overall, the left-skewed EPCs showed marginally greater lag (0.114 larger on average), but this was small compared to the overall amount of variation in the simulations (Fig.4bii).

5 Discussion

Our results shed new light on how the physiological traits of species may impact their responses to climate change. The overall shape of a species environmental performance curve can be expected to have a significant influence and our results allow the identification of a suite of influential features. In this context, our finding that the *direction* of this skew is not relevant to to either the likelihood of population persistence or the range shift lag in our model is particularly surprising. Meta-analyses of the rates of species range shifts have not identified strong trait or taxonomic signals, instead identifying range size and habitat breadth as the most informative predictors (Maclean & Beissinger 2017; Lenoir et al. 2020). If it is assumed that the direction of environmental performance asymmetry is linked to taxonomy, this would align with our results, however data specifying environmental performance curves is not presently available to conduct strong tests.

Our findings contrast with a previous modelling result (Hurford et al. 2019) that found through simulations of a single species IDE model that positively skewed EPCs (with a long tail at high temperatures) were associated with an reduced lags compared to negatively skewed EPCs. Hurford et al. (2019) attributed this result to increased immigration into newly suitable areas from high-density populations near the leading edge. The discordance with our analytic results suggests that this result is an emergent property of at least one of the additional features of their model, likely the possibility for longer range dispersal from areas of high population density. Analytic results will never be able to include the full diversity of process that simulation models can achieve, for example heavy-tailed dispersal models that do not have moment-generating functions (Liu & Kot 2019). Nonetheless the expansion of analytic results is fundamental to building a foundation of expectations for how the natural world will react.

It must be noted that Schrödinger equations are 'true' only in the sense that it is a description of how a system will change given a set of assumptions. In physics, beyond the simplest case of the movement of a hydrogen atom in a vacuum, the complexities of multi-body problems limit the resolution with which predictions can be made. The same is true in ecology, and there are a large number of additional processes that will influence the observed dynamics (Urban et al. 2016). In particular, our model includes a strong role for dispersal not just as a driver of initial colonisation,

but also playing a role in determining population densities through significant mass-effects. Our dispersal term D can be considered a 'displacement' term, and results in a not-insignificant reduction in population density in central areas due to emmigration. Our model is therefore likely to be most directly applicable at local scales where mass effects are more significant than occasional rare long-distance dispersal events. It is important to reiterate that the value of this type of modelling is not wholly derived from accurate correspondences – as much, and sometimes more, insight of ecological value can be derived from mismatches that highlight the fundamental factors. Nonetheless, the replication of our theoretical results to the spatial inhomogeneity and density-dependence that we introduced in our simulation model is heartening. It gives reason to believe that the theory is applicable to real-world systems.

Our approach to modelling temporal variability effectively only modifies the underlying growth curve. It therefore only indirectly captures the impact of discrete stochastic events, that can be highly influential over short time frames relevant to contemporary climate change responses. Further, neither our analytic model or our simulation model explicitly includes interactions between species. Interactions with other species can lead to the 'box-car effect' where competitive interactions slow the rate of advance (Urban et al. 2012; Legault et al. 2020) as well as the potential for extirpation from areas due to the climate-driven arrival of new species. Although the shape of the environmental performance could be attributed to indirect biotic as well as direct influences of the environment, this would not necessarily capture the full dynamic influence of other species, particularly when climate variability is considered (Terry et al. 2021). Models for interacting species within the reaction-diffusion framework have been developed (Cantrell & Cosner 2003, Potapov and Lewis 2014) and incorporating interactions within a moving-environment framework is an interesting future avenue of research. Our model also assumes that species traits are fixed, but species also have the potential to adapt their traits to changing climates through plasticity or evolution (Hoffmann & Sgrò 2011). Trait adaptation can be build directly into the partial differential equation framework (Pease et al. 1989, Chevin et al. 2010), and expectations of interactions between rates of evolution and other key properties is another promising area for future research.

In principle, the parameters in the analytic model could be directly measured for natural populations (Leroux et al. 2013). However, measuring dispersal rates in the field is very chal-

lenging, given the importance of rare, long distance events (Kerr 2020). The rate of dispersal and colonisation of new habitats is fundamentally unpredictable, even under tightly controlled experimental conditions (Melbourne & Hastings 2009) and so there will be hard limits to the expectations of the accuracy of any direct application of the model to a particular species. In our descriptions, we consider $u()$ as being directly a population density (individuals per unit length). However, the same results can apply if instead $u()$ is considered as the density of patches occupied by the population at a location (occupied patches per unit length), in the spirit of metapopulation modelling introduced by Levins (1969). This second interpretation may be more directly amenable to empirical verification or parametrisation using grid-cell occupancy data. Nonetheless our models demonstrate the potential for partial-differential equation models can be used to derive results that are directly relevant to management decisions. We identify that interventions that increase local population size will have the greatest effect on the long-term prospects of a range shifting species species if they are located away from the peak area of performance, in areas where the environmental response is shallower. This stays true regardless of whether this was the 'leading-edge' or 'trailing edge' and can therefore form a possible rule-of-thumb when information is sparse.

Although partial differential equation models of spatial movement have a very rich pedigree within ecology (Fisher 1937; Hastings et al. 2005), our results show how there still remain many results and techniques from the toolbox of quantum physics that can be applied to generate fresh ecological perspectives and more detailed baseline expectations. We use this toolbox to precisely describe the motion of diffuse entities and base our results around the properties of a stable travelling wave. Our analytic framework is therefore orientated around long-term equilibrial solutions that can inform the destination but not the route. There is considerable scope for the analysis of transient dynamics following the start of the perturbation (in this case climate change), which may be more representative of available ecological observations (Hastings 2016). Our work is therefore distinct to the fundamental uncertainty aspects of quantum physics that may be familiar to some readers, although previous authors have suggested those could have ecological applications too (Bull 2015; Real et al. 2017).

6 Acknowledgements

All authors were funded by NERC grant NE/T003510/1.

6.1 Author Contributions

JCDT lead the writing of the manuscript and built the simulation model. AGR derived the original analytic results and the first draft of the supplementary materials. All authors contributed to discussing the results and editing the manuscript.

6.2 Data accessibility statement

This paper uses no empirical data. All code used and simulation results are publicly available at `https://github.com/jcdterry/AnalyticRangeShift_Public` and should the manuscript be accepted will be archived in an appropriate public repository (Zenodo).

7 References

Alexander, J.M., Chalmandrier, L., Lenoir, J., Burgess, T.I., Essl, F., Haider, S., et al. (2018). Lags in the response of mountain plant communities to climate change. Global Change Biology, 24, 563–579.

Berestycki, H., Diekmann, O., Nagelkerke, C.J. & Zegeling, P.A. (2009). Can a species keep pace with a shifting climate? Bulletin of Mathematical Biology.

Brito-Morales, I., García Molinos, J., Schoeman, D.S., Burrows, M.T., Poloczanska, E.S., Brown, C.J., et al. (2018). Climate Velocity Can Inform Conservation in a Warming World. Trends in Ecology and Evolution, 33, 441–457.

Brooker, R.W., Travis, J.M.J., Clark, E.J. & Dytham, C. (2007). Modelling species' range shifts in a changing climate: The impacts of biotic interactions, dispersal distance and the rate of climate change. Journal of Theoretical Biology, 245, 59–65.

Bull, J.W. (2015). Quantum Conservation Biology: A New Ecological Tool. Conservation Letters, 8, 227–229.

Cantrell, R.S. & Cosner, C. (2003). Spatial Ecology via Reaction-Diffusion Equations. Wiley series in mathematical and computational biology. John Wiley & Sons Ltd.

Caswell, H. (2012). Matrix models and sensitivity analysis of populations classified by age and stage: a vec-permutation matrix approach. Theor Ecol, 5, 403–417.

Caswell, H. (2019). Introduction: Sensitivity Analysis – What and Why? In: Sensitivity Analysis: Matrix Methods in Demography and Ecology, Demographic Research Monographs (ed. Caswell, H.). Springer International Publishing, Cham, pp. 3–12.

Chevin, L.-M., Lande, R. & Mace, G.M. (2010). Adaptation, Plasticity, and Extinction in a Changing Environment: Towards a Predictive Theory. PLoS Biol, 8, e1000357.

Elith, J. & Leathwick, J.R. (2009). Species distribution models: Ecological explanation and prediction across space and time. Annual Review of Ecology, Evolution, and Systematics, 40, 677–697.

Fisher, R.A. (1937). THE WAVE OF ADVANCE OF ADVANTAGEOUS GENES. Annals of Eugenics, 7, 355:369.

Harsch, M.A., Phillips, A., Zhou, Y., Leung, M.R., Rinnan, D.S. & Kot, M. (2017). Moving forward: insights and applications of moving-habitat models for climate change ecology. Journal of Ecology, 105, 1169–1181.

Hastings, A. (2016). Timescales and the management of ecological systems. Proceedings of the National Academy of Sciences, 113, 14568–14573.

Hastings, A., Cuddington, K., Davies, K.F., Dugaw, C.J., Elmendorf, S., Freestone, A., et al. (2005). The spatial spread of invasions: New developments in theory and evidence. Ecology Letters, 8, 91–101.

Hoffmann, A.A. & Sgrò, C.M. (2011). Climate change and evolutionary adaptation. Nature, 470, 479–485.

Hurford, A., Cobbold, C.A. & Molnár, P.K. (2019). Skewed temperature dependence affects range and abundance in a warming world. Proceedings of the Royal Society B: Biological Sciences, 286, 20191157.

Kareiva, P. & Shigesada, N. (1983). Analyzing insect movement as a correlated random walk. Oecologia, 56, 234–238.

Kerr, J.T. (2020). Racing against change: Understanding dispersal and persistence to improve

species' conservation prospects. Proceedings of the Royal Society B: Biological Sciences, 287.

Kot, M. & Phillips, A. (2015). Bounds for the critical speed of climate-driven moving-habitat models. Mathematical Biosciences, 262, 65–72.

Legault, G., Bitters, M.E., Hastings, A. & Melbourne, B.A. (2020). Interspecific competition slows range expansion and shapes range boundaries. Proceedings of the National Academy of Sciences, 117, 26854–26860.

Lenoir, J., Bertrand, R., Comte, L., Bourgeaud, L., Hattab, T., Murienne, J., et al. (2020). Species better track climate warming in the oceans than on land. Nature Ecology & Evolution, 4, 1044–1059.

Leroux, S.J., Larrivée, M., Boucher-Lalonde, V., Hurford, A., Zuloaga, J., Kerr, J.T., et al. (2013). Mechanistic models for the spatial spread of species under climate change. Ecological Applications, 23, 815–828.

Levins, R. (1966). The strategy of model building in population biology. American Naturalist, 54, 421–431.

Levins, R. (1969). Some Demographic and Genetic Consequences of Environmental Heterogeneity for Biological Control1. Bulletin of the Entomological Society of America, 15, 237–240.

Li, B., Bewick, S., Shang, J.I.N. & Fagan, W.F. (2014). PERSISTENCE AND SPREAD OF A SPECIES WITH A SHIFTING HABITAT EDGE. SIAM Journal on Applied Mathematics, 74, 1397–1417.

Liu, B.R. & Kot, M. (2019). Accelerating invasions and the asymptotics of fat-tailed dispersal. Journal of Theoretical Biology, 471, 22–41.

Lurgi, M., Brook, B.W., Saltré, F. & Fordham, D.A. (2015). Modelling range dynamics under global change: Which framework and why? Methods in Ecology and Evolution, 6, 247–256.

MacLean, S.A. & Beissinger, S.R. (2017). Species' traits as predictors of range shifts under contemporary climate change: A review and meta-analysis. Global Change Biology, 23, 4094–4105.

Mattis, D.C. (1993). The Many-Body Problem: An Encyclopedia of Exactly Solved Models in One Dimension(3rd Printing with Revisions and Corrections). WORLD SCIENTIFIC.

Melbourne, B.A. & Hastings, A. (2009). Highly Variable Spread Rates in Replicated Biological Invasions: Fundamental Limits to Predictability. Science, 325, 1536–1539.

Morse, P.M. (1929). Diatomic Molecules According to the Wave Mechanics. II. Vibrational Levels. Phys. Rev., 34, 57–64.

Nadeau, C.P., Urban, M.C. & Bridle, J.R. (2017). Climates Past, Present, and Yet-to-Come Shape Climate Change Vulnerabilities. Trends in Ecology & Evolution, 32, 786–800.

Nagasawa, M. (1993). Equivalence of Diffusion and Schrödinger Equations. In: Schrödinger Equations and Diffusion Theory, Monographs in Mathematics (ed. Nagasawa, M.). Birkhäuser, Basel, pp. 89–114.

Parmesan, C. & Yohe, G. (2003). A globally coherent fingerprint of climate change. Nature, 421, 37–42.

Potapov, A.B. & Lewis, M.A. (2004). Climate and competition: The effect of moving range boundaries on habitat invasibility. Bulletin of Mathematical Biology, 66, 975–1008.

Real, R., Márcia Barbosa, A. & Bull, J.W. (2017). Species distributions, quantum theory, and the enhancement of biodiversity measures. Systematic Biology, 66, 453–462.

Rumpf, S.B., Hülber, K., Wessely, J., Willner, W., Moser, D., Gattringer, A., et al. (2019). Extinction debts and colonization credits of non-forest plants in the European Alps. Nature Communications, 10, 1–9.

Savage, V.M., Gillooly, J.F., Brown, J.H., West, G.B. & Charnov, E.L. (2004). Effects of body size and temperature on population growth. American Naturalist, 163, 429–441.

Schrödinger, E. (1926). An Undulatory Theory of the Mechanics of Atoms and Molecules. Phys. Rev., 28, 1049–1070.

Skellam, A.J.G. (1951). Random Dispersal in Theoretical Populations. Biometrika, 38, 196–218.

Strasser, C.A., Neubert, M.G., Caswell, H. & Hunter, C.M. (2012). Contributions of high- and low-quality patches to a metapopulation with stochastic disturbance. Theor Ecol, 5, 167–179.

Svenning, J.C. & Sandel, B. (2013). Disequilibrium vegetation dynamics under future climate change. American Journal of Botany, 100, 1266–1286.

Terry, J.C.D., O'Sullivan, J.D. & Rossberg, A.G. (2021). Synthesising the multiple impacts of climatic variability on community responses to climate change. bioRxiv, 1–31.

Thompson, P.L. & Fronhofer, E.A. (2019). The conflict between adaptation and dispersal for maintaining biodiversity in changing environments. Proceedings of the National Academy of

Sciences of the United States of America, 116, 21061–21067.

Thompson, P.L. & Gonzalez, A. (2017). Dispersal governs the reorganization of ecological networks under environmental change. Nature Ecology & Evolution, 1, 0162.

Urban, M.C., Bocedi, G., Hendry, A.P., Mihoub, J.B., Peer, G., Singer, A., et al. (2016). Improving the forecast for biodiversity under climate change. Science, 353, aad8466.

Urban, M.C., Tewksbury, J.J. & Sheldon, K.S. (2012). On a collision course: competition and dispersal differences create no-analogue communities and cause extinctions during climate change. Proceedings of the Royal Society B: Biological Sciences, 279, 2072–2080.

Yalcin, S. & Leroux, S.J. (2017). Diversity and suitability of existing methods and metrics for quantifying species range shifts. Global Ecology and Biogeography, 26, 609–624.

Zhou, Y. & Kot, M. (2011). Discrete-time growth-dispersal models with shifting species ranges. Theoretical Ecology, 4, 13–25.

Zurell, D., Pollock, L.J. & Thuiller, W. (2018). Do joint species distribution models reliably detect interspecific interactions from co-occurrence data in homogenous environments? Ecography, 41, 1812–1819.

Zurell, D., Thuiller, W., Pagel, J., Cabral, J.S., Münkemüller, T., Gravel, D., et al. (2016). Benchmarking novel approaches for modelling species range dynamics. Global Change Biology, 22, 2651–2664.